Qeios https://doi.org/10.32388/5OFMOA

A simple direct empirical observation of systematic bias of the redshift as a distance indicator

Lior Shamir*
Kansas State University
1701 Platt St
Manhattan, KS 66506, USA

Abstract

Recent puzzling observations such as the H_o tension, large-scale anisotropies, and massive disk galaxies at high redshifts have been challenging the standard cosmological model. While one possible explanation is that the standard model is incomplete, other theories are based on the contention that the redshift model as a distance indicator might be biased. While these theories can explain the recent observations, they are challenged by the absence of a direct empirical reproducible observation that the redshift model can indeed be inconsistent. Here I describe a simple experiment that shows that the spectra of galaxies depend on their rotational velocity relative to the rotational velocity of the Milky Way. Moreover, it shows that the redshift of galaxies that rotate in the same direction relative to the Milky Way is significantly different from the redshift of galaxies that rotate in the opposite direction relative to the Milky Way ($P< 0.006$). Three different datasets are used independently, each one was prepared in a different manner, and all of them show similar redshift bias. A fourth dataset of galaxies from the Southern Galactic pole was also analyzed, and shows similar results. All four datasets are publicly available. While a maximum average Δz of $\sim$0.012 observed with galaxies of relatively low redshift ($z<0.25$) might not seem dramatic, the bias is consistent, and can explain puzzling observations such as the H_o tension.

1 Introduction

Recent observations have shown unexplained tensions and anomalies at cosmological scales. For instance, the H_o determined by the Cosmic Microwave Background (CMB) radiation is different from the H_o determined by using Ia supernovae and the redshift of their host galaxies (Wu and Huterer, 2017; Mörtsell and Dhawan, 2018; Bolejko, 2018; Davis et al., 2019; Pandey et al., 2020; Camarena and Marra, 2020; Di Valentino et al., 2021; Riess et al., 2022). The relatively new JWST provides unprecedented imaging power, showing mature massive disk galaxies at high redshifts where such galaxies are not expected to form due to their young age. In fact, large disk galaxies at unexpectedly high redshifts were identified also before JWST saw first light (Neeleman et al., 2020).

These unexpected observations challenge our understanding of the Universe. If the common distance indicators are complete, the standard cosmological theories are incomplete, or vice versa. Explaining these observations might therefore reinforce the modifications of some of the foundations of cosmology. In addition to theories that shift from the standard cosmological model, other theories are based on the contention that the redshift as used to measure distances at cosmological scales might be an incomplete model (Seshavatharam and Lakshminarayana, 2023; Pletcher, 2023; Gupta, 2023; Lee, 2023). While the assumption that the redshift is not necessarily a complete indicator of the distance can explain these observations without modifying the standard cosmological models, there is no clear reproducible empirical evidence that the redshift might indeed be biased.

The redshift of a luminous moving object is determined by the linear component of the Doppler shift effect. But because galaxies have rotational velocity in addition to their linear velocity, their redshift can also be affected by the rotational velocity, as the rotational velocity of a luminous object does lead to a Doppler shift effect (Marrucci, 2013; Lavery et al., 2014; Liu et al., 2019).

Since the rotational velocity of a galaxy is far smaller than its linear velocity relative to Earth, the rotational velocity component of the Doppler shift is often ignored when determining the distance of a galaxy based on its redshift. But while the Doppler shift effect driven by the rotational velocity of the galaxy is expected to be subtle, that has not yet been tested. It should also be reminded that the physics of galaxy rotation is one of the most provocative observations in nature, and its nature cannot be explained unless making assumptions such as dark matter (Zwicky, 1937; Oort, 1940; Rubin, 1983), modified Newtonian dynamics (Milgrom, 1983, 2007; De Blok and McGaugh, 1998; Sanders, 1998; Sanders and McGaugh, 2002; Swaters et al., 2010; Sanders, 2012; Iocco et al., 2015; Díaz-Saldaña et al., 2018; Falcon, 2021), or other theories (Sanders, 1990; Capozziello and De Laurentis, 2012; Chadwick et al., 2013; Farnes, 2018; Rivera, 2020; Nagao, 2020; Blake, 2021; Gomel and Zimmerman, 2021; Larin, 2022). But despite over a century of research, there is still no single clear proven explanation to the physics of galaxy rotation (Sanders, 1990; Mannheim, 2006; Kroupa, 2012; Kroupa et al., 2012; Kroupa, 2015; Arun et al., 2017; Akerib et al., 2017; Bertone and Tait, 2018; Aprile et al., 2018; Skordis and Złośnik, 2019; Sivaram et al., 2020; Hofmeister and Criss, 2020; Byrd and Howard, 2021), and that phenomenon is still not fully understood. The purpose of this simple experiment is the test the

*lshamir@mtu.edu

impact of the rotational velocity component of galaxies on the Doppler shift effect, and consequently on the redshift as a distance indicator.

2 Data

The experiment is based on one primary dataset, and two additional independent datasets to which the results are compared. The primary dataset includes SDSS DR8 galaxies with spectra sorted by their direction of rotation, as explained and used in (Shamir, 2020b). Instead of using galaxies in the entire SDSS footprint, this experiment is focused on galaxies that rotate in the same direction relative to the Milky Way, and galaxies that rotate in the opposite direction relative to the Milky Way. Therefore, only galaxies that are close to the Galactic pole are used, and the field is limited to the 20×20 degrees centered at the Northern Galactic pole. The analysis included objects with spectra in SDSS DR8 that have an r magnitude of less than 19 and a Petrosian radius of at least 5.5". The redshift of the galaxies in that initial set was limited to z<0.3, and the redshift error was smaller than 10^{-4}. That selection eliminated the possible effect of bad redshift values, which in some cases can be very high and skew the dataset. The initial set of galaxies that meet these criteria in that field was 52,328.

The process by which the galaxies were sorted by their direction of rotation is explained in detail in (Shamir, 2020b), and is similar to the process of annotating galaxies imaged by other telescopes (Shamir, 2016, 2020a, 2022b,f,c; Mcadam et al., 2023; Shamir and McAdam, 2022). In summary, the annotation is done by using the Ganalyzer algorithm (Shamir, 2011), where each galaxy image is transformed into its radial intensity plot such that the value of the pixel at Cartesian coordinates (θ, r) in the radial intensity plot is the median value of the 5×5 pixels at coordinates $(O_x + \sin(\theta) \cdot r, O_y - \cos(\theta) \cdot r)$ in the original galaxy image, where r is the radial distance measured in percentage of the galaxy radius, θ is the polar angle in degrees relative to the galaxy center, and (O_x, O_y) is the coordinates of the galaxy center. A peak detection algorithm is then applied to the rows in the radial intensity plot, and the direction of the peaks determines the direction of the curves of the galaxy arms.

Figure 1 displays examples of the original galaxy images, their radial intensity plots, and the detected peaks. The direction of the curves of the arms is determined by the sign of the slope, given that at least 30 peaks are identified in the radial intensity plot. If less than 30 peaks are identified the galaxy is not used, as its direction of rotation cannot be identified. The algorithm is described with experimental results in (Shamir, 2011), as well as (Shamir, 2020a, 2022b,f,c; Mcadam et al., 2023).

The primary advantage of the algorithm is that its simple "mechanical" nature makes it fully symmetric. Experiments when mirroring the galaxy images lead to identical inverse results compared to when using the original images (Shamir, 2016, 2020a, 2022b,f,c; Mcadam et al., 2023).

After applying the algorithm to the galaxy images, the final dataset included 1,642 galaxies with an identifiable direction of rotation, such that 817 galaxies rotate clockwise, and 825 galaxies rotate counterclockwise. Applying the algorithm to the mirrored images led to an identical inverse dataset. Testing a random subset of 200 galaxies showed that all galaxies were annotated correctly. Figure 2 shows the redshift distribution of the galaxies. The dataset is available at `http://people.cs.ksu.edu/~lshamir/data/zdif_data`. In addition to this dataset, two other previous public datasets were used, as will be described in Section 4.

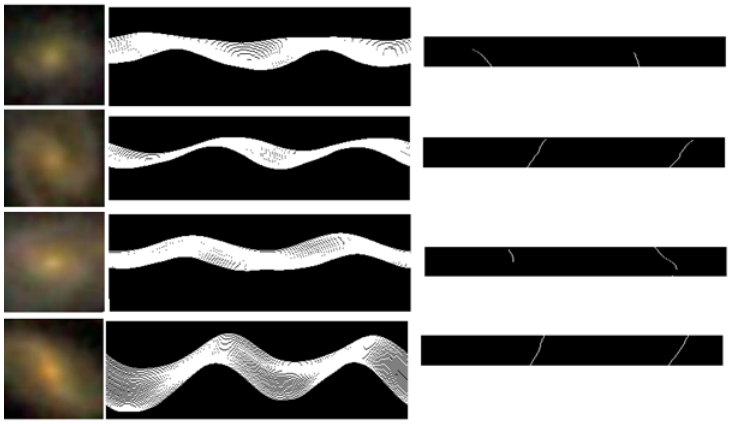

Figure 1: Examples of original galaxy images (left), the radial intensity plot transformations (center), and the peaks detected in the radial intensity plot lines (right).

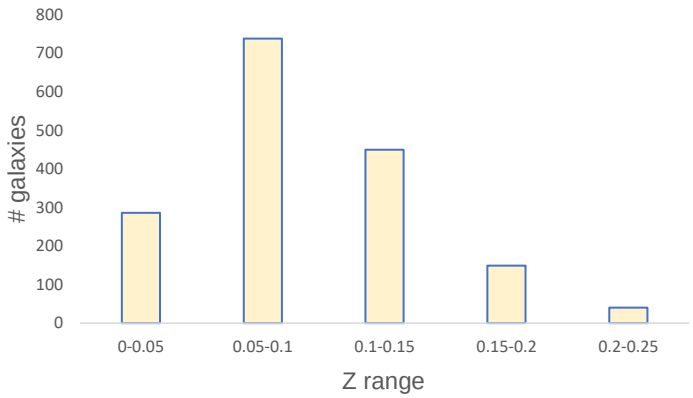

Figure 2: The redshift distribution of the galaxies in the dataset.

3 Results

Table 1 shows the redshift differences in the 20×20 degree field centered at the Northern Galactic pole, as well as the smaller 10×10 degree field. The mean redshift of the galaxies in the dataset described in Section 2 that rotate in the opposite direction relative to the Milky Way (observed from Earth as rotating clockwise) is 0.09545±0.0017, while the mean redshift of the galaxies that rotate in the opposite direction in the same field is 0.08895±0.0016. That shows a Δz of ∼0.0065 between galaxies that rotate in the same direction relative to the Milky Way and galaxies that rotate in the opposite direction relative to the Milky Way. By applying a simple Student t-test, the two-tailed probability that the two means

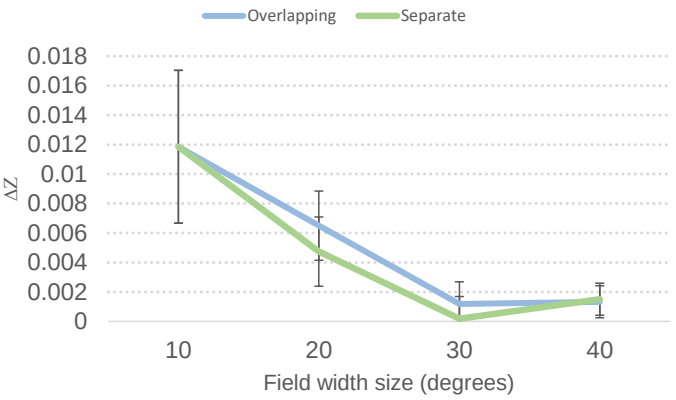

Figure 3: The Δz when the size of the field changes. The analysis was done such that the larger field contains also the galaxies of the smaller field inside it (blue), and also when the galaxies in the smaller field are excluded so that the two fields are orthogonal, and do not have overlapping galaxies (green).

are different by mere chance is (P$\simeq$0.0058).

If the observed difference in redshift is driven by the rotational velocity of the observed galaxy relative to the rotational velocity of the Milky Way, the difference should increase when the observed galaxies are closer to the Galactic pole. As Table 1 shows, Δz indeed increases in the 10×10 field. Despite the lower number of galaxies, the difference is still statistically significant.

Most objects with spectra in SDSS are concentrated in the part of the sky that is close to the Northern Galactic pole. If the redshift difference peaks at the Northern Galactic pole, it is expected that when using galaxies that are more distant from the Galactic pole the redshift difference Δz would decrease. Figure 3 shows the change in Δz when the size of the field centered at the Galactic pole changes.

As the figure shows, the Δz decreases as the field gets larger. That can be explained by the fact that when the field gets larger, it includes more galaxies that are more distant from the Galactic pole. While it does not fully prove a link to the rotational velocity, that observation is in agreement with the contention that the redshift difference is linked to the rotational velocity of the galaxies relative to the rotational velocity of the Milky Way. The figure includes two graphs. The first shows all galaxies inside the field. For instance, when the field size is 20×20 degrees it also includes the galaxies inside the 10×10 degree field centered at the Galactic pole. The other analysis excludes overlapping galaxies, so that a galaxy can only be used in one field. That is, the galaxies in the 20×20 degree field centered at the Galactic pole exclude the galaxies in the 10×10 degree field. That provides analysis with independent sets of galaxies that do not overlap.

Table 2 shows the differences between the flux on the different filters, taken from the specObjAll table in SDSS DR8. The spectrum flux difference shows a consistent difference of $\sim$10% across the different filters. Unlike the redshift, the differences in the flux of the specific filters are not statistically significant, and therefore a definite conclusion about the flux differences cannot be made.

4 Comparison to other datasets

The annotation algorithm used to sort the galaxies by their direction of rotation as discussed in Section 2 is simple and symmetric, and there is no known bias that can prefer the redshift of a certain set of galaxies as annotated by the algorithm. Also, experimenting with the same images when the images were mirrored leads to inverse results, as also shown in detail in (Shamir, 2016, 2020a, 2022b,f,c; Mcadam et al., 2023). To further test for a possible impact of unknown or unexpected biases in the annotation process, two additional annotation methods were used to test whether these algorithms provide different results.

4.1 Comparison to annotations by *Galaxy Zoo*

The first annotation method that was used is the crowdsourcing-based *Galaxy Zoo 1* (Lintott et al., 2008). In *Galaxy Zoo*, anonymous volunteers used a web-based interface to sort galaxy images by their direction of rotation. After several years of work by over 100,000 volunteers, a relatively large set of over $8 \cdot 10^5$ galaxies were annotated. One of the downsides of *Galaxy Zoo* was that in the vast majority of the cases the volunteers who annotated the galaxies made conflicting annotations, and the disagreement between the annotators makes it difficult to use the majority of the galaxies. Another substantial downside is that the annotations were subjected to the bias of human perception, which is very difficult to model and fully understand, challenging the reliability of the annotations as a tool for primary science. Despite these known weaknesses, there is no known human perceptual bias that would associate galaxies with lower redshift to a certain direction of rotation. Therefore, although *Galaxy Zoo* might not necessarily be considered a complete tool when used as the sole dataset, comparing to *Galaxy Zoo* can provide an indication of whether a different annotation method leads to different results shown in Section 3.

Because the annotations of the volunteers often disagree with each other, *Galaxy Zoo* defined the "superclean" criterion as galaxies that 95% of the human annotators agree on the annotation. That is, if 95% of the annotations or more are for a galaxy that rotates clockwise, the annotation is considered "superclean". While these annotations are normally correct, only 1.7% of the galaxies annotated by *Galaxy Zoo 1* meet that criterion. Out of the 667,944 galaxies in the specZoo table in SDSS DR8, just 324 galaxies meet that criterion and are also inside the 20×20 degree field centered at the Northern Galactic pole.

The mean z of the *Galaxy Zoo 1* galaxies that rotate clockwise in that field is 0.073834±0.0041, and the mean z of the galaxies that rotate counterclockwise is 0.068292±0.00348. That shows a Δz of 0.00554, which is similar in both direction and magnitude to the Δz of 0.0065 observed with the dataset described in Section 2. The one-tailed P value for the occurrence of the difference by mere chance is 0.15. That is not statistically significant, and that can be attributed to the small size of the dataset, but the similar Δz in both direction and magnitude shows consistency between the annotation methods. From the 324 galaxies annotated by Galaxy Zoo, 263 were also included in the dataset described in Section 2. The

Table 1: The mean redshift difference of galaxies in 20×20 field centered at the Galactic pole and the 10×10 field centered at the Galactic pole. The P values are the two-tailed P values determined by the standard Student t-test.

Field	# CW	# CCW	Z_{cw}	Z_{ccw}	Δ	t-test P
10×10	204	202	0.0996±0.0036	0.08774±0.0036	0.0118496	0.02
20×20	817	825	0.09545±0.0017	0.08895±0.0016	0.0065	0.0058

Table 2: Flux in different filter galaxies that rotate in the same direction relative to the Milky Way and galaxies that rotate in the opposite direction relative to the Milky Way. The t-test P values are the two-tailed P value.

Band	CW	CCW	Δ	t-test P
spectroFlux_g	25.969±0.8669	28.554±1.0918	-2.585	0.063
spectroFlux_r	53.2433±1.765	58.6214±2.3422	-5.378	0.066
spectroFlux_i	77.4189±2.513	85.0868±3.407	-7.667	0.067

value of the comparison is therefore not by providing a new dataset, but by using a different annotation method that is independent of the method used in Section 2, and therefore not subjected to the same possible unknown or unexpected biases in that method if such exist.

4.2 Comparison to annotations by *SpArcFiRe*

Another dataset that is used is the dataset of SDSS galaxies annotated by the *SpArcFiRe* (Scalable Automated Detection of Spiral Galaxy Arm) algorithm (Davis and Hayes, 2014; Hayes et al., 2017). *SpArcFiRe* is implemented by an open source software [1], and the method is described in detail in (Davis and Hayes, 2014). In summary, the algorithm first identifies arm segments in the galaxy image, and then fits these segments to logarithmic spiral arcs to determine the direction of rotation based on the curves of the arms. One of the advantages of *SpArcFiRe* is that it is not based on data-driven machine learning or deep learning approaches that are difficult to analyze, and is therefore not subjected to the complex biases that are often very difficult to notice (Dhar and Shamir, 2022). The downside of *SpArcFiRe* is that it has an annotation error of about 15% (Mcadam et al., 2023). More importantly, since *SpArcFiRe* is a relatively sophisticated algorithm, it is more difficult to ensure that it is completely symmetric, and in some seldom cases a mirrored galaxy image is not annotated as rotating to the opposite direction compared to the original image. That characteristic of the algorithm is discussed in the appendix of (Hayes et al., 2017). That weakness of the algorithm can be addressed by repeating the analysis twice, such that in the first experiment the original images are used, and in the second experiment the mirrored images are used. Then, the results of the two experiments can be compared. While that practice might not be ideal, it can be used to compare the results to the results shown in Section 3.

The dataset used here is the dataset of spiral galaxies annotated *SpArcFiRe* used in (Mcadam et al., 2023), which is a reproduction of the experiment described in (Hayes et al., 2017). The dataset is available at `https://people.cs.ksu.edu/~lshamir/data/sparcfire`. More details about the dataset are available in (Mcadam et al., 2023). In summary, the dataset was prepared with the original images, and then again with the mirrored galaxy images. The dataset prepared with the original images contains 138,940 galaxies, and the dataset prepared with the mirrored images contains 139,852 galaxies. All of these galaxies have spectra, and therefore can be used to compare the redshift. As before, galaxies with a redshift greater than 0.3 or redshift error greater than 10^{-4} were ignored. Table 3 shows the mean redshift in the 10×10 field centered at the Northern Galactic pole and in the 20×20 field, for both the original images and the mirrored images.

As the table shows, both the original images and the mirrored images show consistent results. These results are also consistent with the results shown in Section 3. The Δz is lower than the Δz observed with the dataset used in Section 3, and that could be due to the certain error rate of the *SpArcFiRe* algorithm, which is expected to weaken the signal as also shown formally in Section 7.1 in (McAdam and Shamir, 2023).

4.3 Comparison to galaxies from the Southern Galactic pole

The data used in the experiments described above was all taken from the Northern hemisphere, and the galaxies it contains are around the Northern Galactic pole. To verify the observed redshift difference, it is also required to test if it exists in the Southern Galactic pole as well. If the observed difference in redshift is also observed in the Southern Galactic pole, it can provide an indication that it is indeed related to the Galactic pole. Since the three experiments above all used data collected by SDSS, using a different telescope can show that the difference is not driven by some unknown or unexpected anomaly in a specific telescope system.

The set of galaxies used for the analysis are galaxies imaged by DECam used in (Shamir, 2021) that had spectroscopic redshift through the Set of Identifications Measurements and Bibliography for Astronomical Data (SIMBAD) database (Wenger et al., 2000). As explained in (Shamir, 2021), DECam galaxy images were acquired through the API of the DESI Legacy Survey server. The galaxy images were then annotated by the Ganalyzer algorithm as described in Section 2, and also in (Shamir, 2021). The entire dataset contains $\sim 8.07{\cdot}10^6$ galaxies, but because only galaxies with spectra in the 20×20 field centered at the Galactic pole are used, the dataset used here is reduced to 3,383 galaxies. The dataset is available at `http://people.cs.ksu.edu/~lshamir/data/zdif_data`.

Table 4 shows the mean redshift of the galaxies that rotate in the same direction relative to the Milky Way and in the opposite direction relative to the Milky Way. Due to the perspective of the observer galaxies that are close to the Southern Galactic pole that rotate in the same direction relative to the Milky Way seem to rotate in the opposite direction compared

[1] https://github.com/waynebhayes/SpArcFiRe

Table 3: The mean redshift of galaxies annotate by the *SpArcFiRe* algorithm. The t-test P values are the one-tailed P value.

Field	# CW	# CCW	Z_{cw}	Z_{ccw}	Δ	t-test P
Original 10×10	710	732	0.07197±0.0015	0.06234±0.0014	0.00963	<0.0001
Mirrored 10×10	728	709	0.06375±0.0014	0.07191±0.0014	-0.00816	<0.0001
Original 20×20	2903	2976	0.07285±0.0007	0.071164±0.0007	0.001686	0.0443
Mirrored 20×20	3003	2914	0.07113±0.0007	0.07271±0.0007	-0.00158	0.0505

to galaxies in the Northern Galactic pole that rotate in the same direction.

As the table shows, the redshift differences are statistically significant in both fields, and increases when the galaxies are closer to the Galactic pole. These results are in good agreement with the results shown with galaxies located around the Northern Galactic pole. The table also shows that the mean redshift is higher compared to the mean redshift observed with SDSS. That difference can be expected due to the superior imaging power of DECam compared to SDSS, allowing DECam to image galaxies at deeper redshifts.

5 Conclusion

Recent puzzling observations such as the H_o tension and large disk galaxies at high redshifts have been challenging cosmology. Explaining such observations requires us to assume that either the standard cosmological models are incomplete, or that the redshift as a model of distance is incomplete. This study shows the first direct observational evidence of bias in the redshift as a distance indicator. While the bias can also be attributed to the algorithm that selects spectroscopic targets, it is difficult to think of how that algorithm could be affected by the direction of rotation relative to the Milky Way. Also, if the target selection algorithm has such unknown and complex bias, that bias is expected to be consistent throughout the sky, and is not expected to change based on the angular distance of the galaxy from the Galactic pole, or flip when analyzing galaxies from the opposite side of the Galactic pole. The fact that two different telescope systems show similar results further reduces the possibility that the results are driven by an unknown anomaly in the selection algorithm of the spectroscopic surveys.

Another possible explanation for the observation is an unexpected anomaly in the geometry of the Universe and its large-scale structure. If the redshifts represent the accurate distances of the galaxies, and are not affected by their rotational velocity, the galaxies form a cosmological-scale structure formed by the alignment in the direction of rotation of the galaxies, and peaks around the Galactic pole. That explanation, however, requires the modification of the standard cosmological model and the fundamental assumptions it is based on (Aluri et al., 2023). As discussed also in (Shamir, 2022b,a,d,c,e), the observation of such large-scale structure that forms a cosmological-scale axis is aligned with alternative theories such as dipole cosmology (Allahyari et al., 2023; Krishnan et al., 2023), or theories that assume a rotating universe such as Black Hole Cosmology (Pathria, 1972; Stuckey, 1994; Easson and Brandenberger, 2001; Seshavatharam, 2010; Popławski, 2010; Christillin, 2014; Dymnikova, 2019; Chakrabarty et al., 2020; Popławski, 2021; Seshavatharam and Lakshminarayana, 2022; Gaztanaga, 2022a,b) which is also linked to holographic universe (Susskind, 1995; Bak and Rey, 2000; Bousso, 2002; Myung, 2005; Hu and Ling, 2006; Rinaldi et al., 2022). In that case, the alignment of such hypothetical axis with the Galactic pole is a coincidence.

The experiments described here use galaxies with clear shape, and therefore is limited to a relatively low redshift of $z < 0.25$. Deeper and larger datasets of clear galaxies with spectra such as the data provided by the Dark Energy Spectroscopic Instrument (DESI) will allow a higher resolution profiling of the observed anomaly in higher redshift ranges. While the observations do not explain directly the existence of early massive disk galaxies, they demonstrate that the redshift model might be incomplete. In that case, the existence of such galaxies can be explained without the need to modify the standard cosmological models.

The results shown here might also provide an indication that the H_o tension can be explained by the slight differences in the redshift. While H_o anisotropy has been reported in the past (Krishnan et al., 2022; Cowell et al., 2022; McConville and Colgain, 2023; Aluri et al., 2023), its nature is still unclear. Differences in the redshift that are based on the rotational velocity of the galaxies relative to the Milky Way can explain the H_o anisotropy, and potentially also the H_o tension.

If the rotational velocity of Ia supernovae and their host galaxies relative to the Milky Way affect their estimated distance, when the rotational velocity relative to the Milky Way is normalized the H_o tension is expected to be resolved. That is, when using just galaxies that rotate in the same direction relative to the Milky Way, the computed H_o should be similar to the H_o determined by the CMB. Table 5 shows the H_o computed when using the *SH0ES* collection of Ia supernovae as described in (Khetan et al., 2021), with the open source and data `https://github.com/nanditakhetan/SBF_SNeIa_H0`. The table also shows the same experiment when using just galaxies that rotate in the same direction relative to the Milky Way, and when using galaxies that rotate in the opposite direction relative to the Milky Way. The experiment is described in (McAdam and Shamir, 2023).

As the table shows, when using the galaxies regardless of the direction of their rotational velocity the H_o is $\sim$73.76 $km/sMpc^{-1}$, which is similar to the value reported in (Khetan et al., 2021), and in tension with the H_o determined by the CMB. When limiting the SH0ES collection to galaxies that rotate in the same direction relative to the Milky Way, H_o drops to $\sim$69.05 $km/sMpc^{-1}$, reducing the tension with the CMB. Although certain tension with the CMB still exists, the galaxies are not exactly at the Galactic pole, their inclination is not exactly 90^o, and their rotational velocity is

Table 4: The mean redshift of galaxies in 20×20 field and the 10×10 field centered at the Southern Galactic pole. The P values are the one-tailed Student t-test P values.

Field	# CW	# CCW	Z_{cw}	Z_{ccw}	Δ	t-test P
10×10	414	376	0.1270±0.0025	0.1352±0.0027	0.0082	0.018
20×20	1702	1681	0.1273±0.0014	0.1317±0.0013	0.0044	0.008

Rotation direction	#	H_o	3% error range	SD
All	96	73.758	70.193-77.404	1.943
Same direction	22	69.049	62.955-76.005	3.42
Opposite direction	36	74.182	68.758-79.915	3.2

Table 5: The H_o when using *SH0ES* supernovae, the H_o when using a subset of galaxies that rotate in the same direction relative to the Milky Way, and the H_o when using galaxies that rotate in the opposite direction relative to the Milky Way.

not identical to the rotational velocity of the Milky Way, and therefore the H_o is not expected to be fully identical to the H_o computed with the CMB. When using galaxies that rotate in the opposite direction relative to the Milky Way, not only that the H_o does not decrease, but it increases to make the tension with the CMB stronger.

Since the lower number of galaxies increases the error of the computed H_o, the results shown in Table 5 cannot provide a clear proof, but they are consistent with the contention that the possible slight differences caused by the rotational velocity of the observed galaxies might be linked to the H_o tension. Further analysis with larger sets than *SH0ES* might be needed to better understand whether such a link exists. If the rotational velocity affects distance indicators such as the redshift, observations such as deep fields imaged by space-based telescopes might be more informative when the field is close to the Galactic pole, allowing to separate some of the observed galaxies by their rotational velocity relative to the Milky Way.

The observed Δz between galaxies with opposite rotational velocities as shown here is between around 0.0065 to 0.012. If that difference is due to the rotational velocity, that difference corresponds to a velocity of between roughly 2,000 to 3,600 km·s^{-1}. That is about 5 to 8 times the rotational velocity of the Milky Way compared to the observed galaxies, which is $2 \cdot 220 =\sim 440$ km·s^{-1}, assuming that the observed galaxies have the same rotational velocity as the Milky Way. That velocity difference is in good agreement with the velocity difference predicted in (Shamir, 2020a) by using analysis of the photometric differences between galaxies rotating with or against the rotational velocity of the Milky Way. That analysis was based on the expected and observed differences in the total flux of galaxies that rotate in the same direction relative to the Milky Way and the flux of galaxies that rotate in the opposite direction. Based on the expected flux difference due to the Doppler shift driven by the rotational velocity as shown in (Loeb and Gaudi, 2003), it was predicted that light emitted from the observed galaxies agrees with a rotational velocity that is 5-10 times faster than the rotational velocity of the Milky Way (Shamir, 2020a; McAdam and Shamir, 2023). These predictions are close to the results of comparing the redshift as done here.

There is no immediate physical explanation for the difference between the redshifts of galaxies that rotate with or against the direction of rotation of the Milky Way. While a certain difference is expected, the magnitude of the difference is expected to be far smaller given the rotational velocity of the Milky Way. The observed redshift difference, if indeed linked to the rotational velocity of the Milky Way and the observed galaxies, corresponds to a much higher rotational velocity than the ∼220 km·s^{-1} of the Milky Way. On the other hand, the physics of galaxy rotation is one of the most puzzling phenomena in nature, and despite over a century of research it is still not fully understood (Opik, 1922; Babcock, 1939; Oort, 1940; Rubin and Ford Jr, 1970; Rubin et al., 1978, 1980, 1985; Sanders, 1990; Sofue and Rubin, 2001; Mannheim, 2006; Kroupa, 2012; Kroupa et al., 2012; Kroupa, 2015; Arun et al., 2017; Akerib et al., 2017; Bertone and Tait, 2018; Aprile et al., 2018; Skordis and Złośnik, 2019; Sivaram et al., 2020; Hofmeister and Criss, 2020; Byrd and Howard, 2021). Due to the unexplained tensions in cosmology, the unknown physics of galaxy rotation should be considered as a factor that can be associated with these tensions and explain them.

References

Akerib, D. S., Alsum, S., Araújo, H. M., Bai, X., Bailey, A. J., Balajthy, J., Beltrame, P., Bernard, E. P., Bernstein, A., Biesiadzinski, T. P., Boulton, E. M., Bramante, R., Brás, P., Byram, D., Cahn, S. B., Carmona-Benitez, M. C., Chan, C., Chiller, A. A., Chiller, C., Currie, A., Cutter, J. E., Davison, T. J. R., Dobi, A., Dobson, J. E. Y., Druszkiewicz, E., Edwards, B. N., Faham, C. H., Fiorucci, S., Gaitskell, R. J., Gehman, V. M., Ghag, C., Gibson, K. R., Gilchriese, M. G. D., Hall, C. R., Hanhardt, M., Haselschwardt, S. J., Hertel, S. A., Hogan, D. P., Horn, M., Huang, D. Q., Ignarra, C. M., Ihm, M., Jacobsen, R. G., Ji, W., Kamdin, K., Kazkaz, K., Khaitan, D., Knoche, R., Larsen, N. A., Lee, C., Lenardo, B. G., Lesko, K. T., Lindote, A., Lopes, M. I., Manalaysay, A., Mannino, R. L., Marzioni, M. F., McKinsey, D. N., Mei, D.-M., Mock, J., Moongweluwan, M., Morad, J. A., Murphy, A. S. J., Nehrkorn, C., Nelson, H. N., Neves, F., O'Sullivan, K., Oliver-Mallory, K. C., Palladino, K. J., Pease, E. K., Phelps, P., Reichhart, L., Rhyne, C., Shaw, S., Shutt, T. A., Silva, C., Solmaz, M., Solovov, V. N., Sorensen, P., Stephenson, S., Sumner, T. J., Szydagis, M., Taylor, D. J., Taylor, W. C., Tennyson, B. P., Terman, P. A., Tiedt, D. R., To, W. H., Tripathi, M., Tvrznikova, L., Uvarov, S., Verbus, J. R., Webb, R. C., White, J. T., Whitis, T. J., Witherell, M. S., Wolfs, F. L. H., Xu, J., Yazdani, K., Young, S. K., and Zhang, C. (2017). Results from a search for dark matter in the complete lux exposure. *Phys. Rev. Lett.*, 118:021303.

Allahyari, A., Ebrahimian, E., Mondol, R., and Sheikh-

Jabbari, M. (2023). Big bang in dipole cosmology. *arXiv:2307.15791*.

Aluri, P. K., Cea, P., Chingangbam, P., Chu, M.-C., Clowes, R. G., Hutsemékers, D., Kochappan, J. P., Krasiński, A., Lopez, A. M., Liu, L., Martens, N. C. M., Martins, C. J. A. P., Migkas, K., Colgáin, E. ., Pranav, P., Shamir, L., Singal, A. K., Sheikh-Jabbari, M. M., Wagner, J., Wang, S.-J., Wiltshire, D. L., Yeung, S., Yin, L., and Zhao, W. (2023). Is the observable universe consistent with the cosmological principle? *Classical and Quantum Gravity*, 40(9):094001.

Aprile, E., Aalbers, J., Agostini, F., Alfonsi, M., Althueser, L., Amaro, F. D., Anthony, M., Arneodo, F., Baudis, L., Bauermeister, B., Benabderrahmane, M. L., Berger, T., Breur, P. A., Brown, A., Brown, A., Brown, E., Bruenner, S., Bruno, G., Budnik, R., Capelli, C., Cardoso, J. M. R., Cichon, D., Coderre, D., Colijn, A. P., Conrad, J., Cussonneau, J. P., Decowski, M. P., de Perio, P., Di Gangi, P., Di Giovanni, A., Diglio, S., Elykov, A., Eurin, G., Fei, J., Ferella, A. D., Fieguth, A., Fulgione, W., Gallo Rosso, A., Galloway, M., Gao, F., Garbini, M., Geis, C., Grandi, L., Greene, Z., Qiu, H., Hasterok, C., Hogenbirk, E., Howlett, J., Itay, R., Joerg, F., Kaminsky, B., Kazama, S., Kish, A., Koltman, G., Landsman, H., Lang, R. F., Levinson, L., Lin, Q., Lindemann, S., Lindner, M., Lombardi, F., Lopes, J. A. M., Mahlstedt, J., Manfredini, A., Marrodán Undagoitia, T., Masbou, J., Masson, D., Messina, M., Micheneau, K., Miller, K., Molinario, A., Morå, K., Murra, M., Naganoma, J., Ni, K., Oberlack, U., Pelssers, B., Piastra, F., Pienaar, J., Pizzella, V., Plante, G., Podviianiuk, R., Priel, N., Ramírez García, D., Rauch, L., Reichard, S., Reuter, C., Riedel, B., Rizzo, A., Rocchetti, A., Rupp, N., dos Santos, J. M. F., Sartorelli, G., Scheibelhut, M., Schindler, S., Schreiner, J., Schulte, D., Schumann, M., Scotto Lavina, L., Selvi, M., Shagin, P., Shockley, E., Silva, M., Simgen, H., Thers, D., Toschi, F., Trinchero, G., Tunnell, C., Upole, N., Vargas, M., Wack, O., Wang, H., Wang, Z., Wei, Y., Weinheimer, C., Wittweg, C., Wulf, J., Ye, J., Zhang, Y., and Zhu, T. (2018). Dark matter search results from a one ton-year exposure of xenon1t. *Phys. Rev. Lett.*, 121:111302.

Arun, K., Gudennavar, S., and Sivaram, C. (2017). Dark matter, dark energy, and alternate models: A review. *Advances in Space Research*, 60(1):166–186.

Babcock, H. W. (1939). The rotation of the andromeda nebula. *Lick Observatory Bulletin*, 19:41–51.

Bak, D. and Rey, S.-J. (2000). Holographic principle and string cosmology. *Classical and Quantum Gravity*, 17(1):L1.

Bertone, G. and Tait, T. M. (2018). A new era in the search for dark matter. *Nature*, 562(7725):51–56.

Blake, B. C. (2021). Relativistic beaming of gravity and the missing mass problem. *Bulletin of the American Physical Society*, page B17.00002.

Bolejko, K. (2018). Emerging spatial curvature can resolve the tension between high-redshift cmb and low-redshift distance ladder measurements of the hubble constant. *Physical Review D*, 97(10):103529.

Bousso, R. (2002). The holographic principle. *Reviews of Modern Physics*, 74(3):825.

Byrd, G. and Howard, S. (2021). Spiral galaxies when disks dominate their halos (using arm pitches and rotation curves). *Journal of the Washington Academy of Sciences*, 107(1):1.

Camarena, D. and Marra, V. (2020). Local determination of the hubble constant and the deceleration parameter. *Physical Review Research*, 2(1):013028.

Capozziello, S. and De Laurentis, M. (2012). The dark matter problem from f (r) gravity viewpoint. *Annalen der Physik*, 524(9-10):545–578.

Chadwick, E. A., Hodgkinson, T. F., and McDonald, G. S. (2013). Gravitational theoretical development supporting mond. *Physical Review D*, 88(2):024036.

Chakrabarty, H., Abdujabbarov, A., Malafarina, D., and Bambi, C. (2020). A toy model for a baby universe inside a black hole. *European Physical Journal C*, 80(1909.07129):1–10.

Christillin, P. (2014). The machian origin of linear inertial forces from our gravitationally radiating black hole universe. *The European Physical Journal Plus*, 129(8):1–3.

Cowell, J. A., Dhawan, S., and Macpherson, H. J. (2022). Potential signature of a quadrupolar hubble expansion in pantheon+ supernovae. *arXiv:2212.13569*.

Davis, D. R. and Hayes, W. B. (2014). SpArcFiRe: Scalable Automated Detection of Spiral Galaxy Arm Segments. *Astrophysical Journal*, 790(2):87.

Davis, T. M., Hinton, S. R., Howlett, C., and Calcino, J. (2019). Can redshift errors bias measurements of the hubble constant? *Monthly Notices of the Royal Astronomical Society*, 490(2):2948–2957.

De Blok, W. and McGaugh, S. (1998). Testing modified newtonian dynamics with low surface brightness galaxies: rotation curve fits. *Astrophysical Journal*, 508(1):132.

Dhar, S. and Shamir, L. (2022). Systematic biases when using deep neural networks for annotating large catalogs of astronomical images. *Astronomy and Computing*, 38:100545.

Di Valentino, E., Mena, O., Pan, S., Visinelli, L., Yang, W., Melchiorri, A., Mota, D. F., Riess, A. G., and Silk, J. (2021). In the realm of the hubble tension—a review of solutions. *Classical and Quantum Gravity*, 38(15):153001.

Díaz-Saldaña, I., López-Domínguez, J., and Sabido, M. (2018). On emergent gravity, black hole entropy and galactic rotation curves. *Physics of the Dark Universe*, 22:147–151.

Dymnikova, I. (2019). Universes inside a black hole with the de sitter interior. *Universe*, 5(5):111.

Easson, D. A. and Brandenberger, R. H. (2001). Universe generation from black hole interiors. *Journal of High Energy Physics*, 2001(06):024.

Falcon, N. (2021). A large-scale heuristic modification of newtonian gravity as an alternative approach to dark energy and dark matter. *Journal of Astrophysics and Astronomy*, 42(2):1–13.

Farnes, J. S. (2018). A unifying theory of dark energy and dark matter: Negative masses and matter creation within a modified λcdm framework. *Astronomy & Astrophysics*, 620:A92.

Gaztanaga, E. (2022a). The black hole universe, part i. *Symmetry*, 14(9):1849.

Gaztanaga, E. (2022b). The black hole universe, part ii. *Symmetry*, 14(10):1984.

Gomel, R. and Zimmerman, T. (2021). The effects of inertial forces on the dynamics of disk galaxies. *Galaxies*, 9(2):34.

Gupta, R. (2023). Jwst early universe observations and λcdm cosmology. *Monthly Notices of the Royal Astronomical Society*, page stad2032.

Hayes, W. B., Davis, D., and Silva, P. (2017). On the nature and correction of the spurious s-wise spiral galaxy winding bias in galaxy zoo 1. *Monthyl Notices of the Royal Astronomical Society*, 466(4):3928–3936.

Hofmeister, A. M. and Criss, R. E. (2020). Debate on the physics of galactic rotation and the existence of dark matter.

Hu, B. and Ling, Y. (2006). Interacting dark energy, holographic principle, and coincidence problem. *Physical Review D*, 73(12):123510.

Iocco, F., Pato, M., and Bertone, G. (2015). Testing modified newtonian dynamics in the milky way. *Physical Review D*, 92(8):084046.

Khetan, N., Izzo, L., Branchesi, M., Wojtak, R., Cantiello, M., Murugeshan, C., Agnello, A., Cappellaro, E., Della Valle, M., Gall, C., Hjorth, J., Benetti, S., Brocato, E., Burke, J., Hiramatsu, D., Howell, D. A., Tomasella, L., and Valenti, S. (2021). A new measurement of the hubble constant using type ia supernovae calibrated with surface brightness fluctuations. *Astronomy & Astrophysics*, 647:A72.

Krishnan, C., Mohayaee, R., Colgáin, E. Ó., Sheikh-Jabbari, M., and Yin, L. (2022). Hints of flrw breakdown from supernovae. *Physical Review D*, 105(6):063514.

Krishnan, C., Mondol, R., and Sheikh-Jabbari, M. (2023). Dipole cosmology: the copernican paradigm beyond flrw. *Journal of Cosmology and Astroparticle Physics*, 2023(07):020.

Kroupa, P. (2012). The dark matter crisis: falsification of the current standard model of cosmology. *Publications of the Astronomical Society of Australia*, 29(4):395–433.

Kroupa, P. (2015). Galaxies as simple dynamical systems: observational data disfavor dark matter and stochastic star formation. *Canadian Journal of Physics*, 93(2):169–202.

Kroupa, P., Pawlowski, M., and Milgrom, M. (2012). The failures of the standard model of cosmology require a new paradigm. *International Journal of Modern Physics D*, 21(14):1230003.

Larin, S. A. (2022). Towards the explanation of flatness of galaxies rotation curves. *Universe*, 8(12):632.

Lavery, M. P., Barnett, S. M., Speirits, F. C., and Padgett, M. J. (2014). Observation of the rotational doppler shift of a white-light, orbital-angular-momentum-carrying beam backscattered from a rotating body. *Optica*, 1(1):1–4.

Lee, S. (2023). The cosmological evolution condition of the planck constant in the varying speed of light models through adiabatic expansion. *Physics of the Dark Universe*, page 101286.

Lintott, C. J., Schawinski, K., Slosar, A., Land, K., Bamford, S., Thomas, D., Raddick, M. J., Nichol, R. C., Szalay, A., Andreescu, D., et al. (2008). Galaxy zoo: morphologies derived from visual inspection of galaxies from the sloan digital sky survey. *Monthly Notices of the Royal Astronomical Society*, 389(3):1179–1189.

Liu, B., Chu, H., Giddens, H., Li, R., and Hao, Y. (2019). Experimental observation of linear and rotational doppler shifts from several designer surfaces. *Scientific Reports*, 9(1):8971.

Loeb, A. and Gaudi, B. S. (2003). Periodic flux variability of stars due to the reflex doppler effect induced by planetary companions. *Astrophysical Journal Letters*, 588(2):L117.

Mannheim, P. D. (2006). Alternatives to dark matter and dark energy. *Progress in Particle and Nuclear Physics*, 56(2):340–445.

Marrucci, L. (2013). Spinning the doppler effect. *Science*, 341(6145):464–465.

McAdam, D. and Shamir, L. (2023). Asymmetry between galaxy apparent magnitudes shows a possible tension between physical properties of galaxies and their rotational velocity. *Symmetry*, 15(6):1190.

Mcadam, D., Shamir, L., et al. (2023). Reanalysis of the spin direction distribution of galaxy zoo sdss spiral galaxies. *Advances in Astronomy*, 2023.

McConville, R. and Colgain, E. (2023). Anisotropic distance ladder in pantheon+ supernovae. *arXiv:2304.02718*.

Milgrom, M. (1983). A modification of the newtonian dynamics as a possible alternative to the hidden mass hypothesis. *Astrophysical Journal*, 270:365–370.

Milgrom, M. (2007). Mond and the mass discrepancies in tidal dwarf galaxies. *Astrophysical Journal Letters*, 667(1):L45.

Mörtsell, E. and Dhawan, S. (2018). Does the hubble constant tension call for new physics? *Journal of Cosmology and Astroparticle Physics*, 2018(09):025.

Myung, Y. S. (2005). Holographic principle and dark energy. *Physics Letters B*, 610(1-2):18–22.

Nagao, S. (2020). Galactic evolution showing a constant circulating speed of stars in a galactic disc without requiring dark matter. *Reports in Advances of Physical Sciences*, 4(02):2050004.

Neeleman, M., Prochaska, J. X., Kanekar, N., and Rafelski, M. (2020). A cold, massive, rotating disk galaxy 1.5 billion years after the big bang. *Nature*, 581(7808):269–272.

Oort, J. H. (1940). Some problems concerning the structure and dynamics of the galactic system and the elliptical nebulae ngc 3115 and 4494. *Astrophysical Journal*, 91:273.

Opik, E. (1922). An estimate of the distance of the andromeda nebula. *Astrophysical Journal*, 55.

Pandey, S., Raveri, M., and Jain, B. (2020). Model independent comparison of supernova and strong lensing cosmography: Implications for the hubble constant tension. *Physical Review D*, 102(2):023505.

Pathria, R. (1972). The universe as a black hole. *Nature*, 240(5379):298–299.

Pletcher, A. E. (2023). Why mature galaxies seem to have filled the universe shortly after the big bang. *Qeios*, page 10.32388/2X1GDL.2.

Popławski, N. J. (2010). Radial motion into an einstein–rosen bridge. *Physics Letters B*, 687(2-3):110–113.

Popławski, N. J. (2021). A nonsingular, anisotropic universe in a black hole with torsion and particle production. *General Relativity and Gravitation*, 53(2):1–14.

Riess, A. G., Yuan, W., Macri, L. M., Scolnic, D., Brout, D., Casertano, S., Jones, D. O., Murakami, Y., Anand, G. S., Breuval, L., et al. (2022). A comprehensive measurement of the local value of the hubble constant with 1 km s- 1 mpc- 1 uncertainty from the hubble space telescope and the sh0es team. *Astrophysical Journal Letters*, 934(1):L7.

Rinaldi, E., Han, X., Hassan, M., Feng, Y., Nori, F., McGuigan, M., and Hanada, M. (2022). Matrix-model simulations using quantum computing, deep learning, and lattice monte carlo. *PRX Quantum*, 3(1):010324.

Rivera, P. C. (2020). An alternative model of rotation curve that explains anomalous orbital velocity, mass discrepancy and structure of some galaxies. *American Journal of Astronomy and Astrophysics*, 7(4):73–79.

Rubin, V. C. (1983). The rotation of spiral galaxies. *Science*, 220(4604):1339–1344.

Rubin, V. C., Burstein, D., Ford Jr, W. K., and Thonnard, N. (1985). Rotation velocities of 16 sa galaxies and a comparison of sa, sb, and sc rotation properties. *Astrophysical Journal*, 289:81–98.

Rubin, V. C. and Ford Jr, W. K. (1970). Rotation of the andromeda nebula from a spectroscopic survey of emission regions. *Astrophysical Journal*, 159:379.

Rubin, V. C., Ford Jr, W. K., and Thonnard, N. (1978). Extended rotation curves of high-luminosity spiral galaxies. iv-systematic dynamical properties, sa through sc. *Astrophysical Journal*, 225:L107–L111.

Rubin, V. C., Ford Jr, W. K., and Thonnard, N. (1980). Rotational properties of 21 sc galaxies with a large range of luminosities and radii, from ngc 4605/r= 4kpc/to ugc 2885/r= 122 kpc. *Astrophysical Journal*, 238:471–487.

Sanders, R. (1990). Mass discrepancies in galaxies: dark matter and alternatives. *The Astronomy and Astrophysics Review*, 2(1):1–28.

Sanders, R. (1998). The virial discrepancy in clusters of galaxies in the context of modified newtonian dynamics. *Astrophysical Journal Letters*, 512(1):L23.

Sanders, R. (2012). Ngc 2419 does not challenge modified newtonian dynamics. *Monthly Notices of the Royal Astronomical Society*, 419(1):L6–L8.

Sanders, R. H. and McGaugh, S. S. (2002). Modified newtonian dynamics as an alternative to dark matter. *Annual Review of Astronomy and Astrophysics*, 40(1):263–317.

Seshavatharam, U. (2010). Physics of rotating and expanding black hole universe. *Progress in Physics*, 2:7–14.

Seshavatharam, U. S. and Lakshminarayana, S. (2023). A rotating model of a light speed expanding hubble-hawking universe. *Physical Sciences Forum*, 7(1):43.

Seshavatharam, U. V. S. and Lakshminarayana, S. (2022). Concepts and results of a practical model of quantum cosmology: Light speed expanding black hole cosmology. *Mapana Journal of Sciences*, 21(2).

Shamir, L. (2011). Ganalyzer: A tool for automatic galaxy image analysis. *Astrophysical Journal*, 736(2):141.

Shamir, L. (2016). Asymmetry between galaxies with clockwise handedness and counterclockwise handedness. *Astrophysical Journal*, 823(1):32.

Shamir, L. (2020a). Asymmetry between galaxies with different spin patterns: A comparison between cosmos, sdss, and pan-starrs. *Open Astronomy*, 29(1):15–27.

Shamir, L. (2020b). Patterns of galaxy spin directions in sdss and pan-starrs show parity violation and multipoles. *Astrophysics & Space Science*, 365:136.

Shamir, L. (2021). Large-scale asymmetry in galaxy spin directions: evidence from the southern hemisphere. *Publications of the Astronomical Society of Australia*, 38:e037.

Shamir, L. (2022a). Analysis of $\sim 10^6$ spiral galaxies from four telescopes shows large-scale patterns of asymmetry in galaxy spin directions. *Advances in Astronomy*, 2022:8462363.

Shamir, L. (2022b). Analysis of spin directions of galaxies in the desi legacy survey. *Monthly Notices of the Royal Astronomical Society*, 516(2):2281–2291.

Shamir, L. (2022c). Asymmetry in galaxy spin directions - analysis of data from des and comparison to four other sky surveys. *Universe*, 8:8.

Shamir, L. (2022d). Large-scale asymmetry in galaxy spin directions: analysis of galaxies with spectra in des, sdss, and desi legacy survey. *Astronomical Notes*, 343(6-7):e20220010.

Shamir, L. (2022e). A possible large-scale alignment of galaxy spin directions - analysis of 10 datasets from sdss, pan-starrs, and hst. *New Astronomy*, 95:101819.

Shamir, L. (2022f). Using 3d and 2d analysis for analyzing large-scale asymmetry in galaxy spin directions. *PASJ*, 74(5):1114–1130.

Shamir, L. and McAdam, D. (2022). A possible tension between galaxy rotational velocity and observed physical properties. *arXiv:2212.04044*.

Sivaram, C., Arun, K., and Rebecca, L. (2020). Mond, mong, morg as alternatives to dark matter and dark energy, and consequences for cosmic structures. *Journal of Astrophysics and Astronomy*, 41(1):1–6.

Skordis, C. and Złośnik, T. (2019). Gravitational alternatives to dark matter with tensor mode speed equaling the speed of light. *Physical Review D*, 100(10):104013.

Sofue, Y. and Rubin, V. (2001). Rotation curves of spiral galaxies. *Annual Review of Astronomy and Astrophysics*, 39:137–174.

Stuckey, W. (1994). The observable universe inside a black hole. *American Journal of Physics*, 62(9):788–795.

Susskind, L. (1995). The world as a hologram. *Journal of Mathematical Physics*, 36(11):6377–6396.

Swaters, R., Sanders, R., and McGaugh, S. (2010). Testing modified newtonian dynamics with rotation curves of dwarf and low surface brightness galaxies. *Astrophysical Journal*, 718(1):380.

Wenger, M., Ochsenbein, F., Egret, D., Dubois, P., Bonnarel, F., Borde, S., Genova, F., Jasniewicz, G., Laloë, S., Lesteven, S., et al. (2000). The simbad astronomical database-the cds reference database for astronomical objects. *Astronomy and Astrophysics Supplement Series*, 143(1):9–22.

Wu, H.-Y. and Huterer, D. (2017). Sample variance in the local measurements of the hubble constant. *Monthly Notices of the Royal Astronomical Society*, 471(4):4946–4955.

Zwicky, F. (1937). On the masses of nebulae and of clusters of nebulae. *Astrophysical Journal*, 86:217.